Available online at www.sciencedirect.com
SCIENCE DIRECT®
Journal of Food Engineering 71 (2005) 345–353
JOURNAL OF FOOD ENGINEERING
www.elsevier.com/locate/jfoodeng

Rotary disc atomisation for microencapsulation applications—prediction of the particle trajectories

E. Teunou *, D. Poncelet

Département de Génie des Procédés Alimentaires, École Nationale d'Ingénieurs des techniques des Industries Agricoles et Alimentaires, Rue de la Géraudière, BP 82225, 44322 NANTES Cedex 3, France

Received 14 April 2004; accepted 24 October 2004
Available online 24 December 2004

Abstract

Disintegration of a liquid by a rotating disc is a technique that has been widely used in spray drying, cooling or freezing for atomisation of the liquid into fine droplets before drying or freezing. This technique is applied today for microencapsulation, which is a promising method to protect the core material, improve the product characteristics and functionalities. It is actually one of the few methods that can be economically applied for microencapsulation in food industries. For this purpose, the structure and the quality of the capsules are determining factors in guaranteeing the properties of the capsules. The capsules, in this case, must be collected in a gentle way, and the trajectory of the capsules, which is the objective of this paper, must be determined. So, paraffin microbeads (1–1000 μm in diameter) were produced by disintegration of hot liquid paraffin with a rotating disc. The trajectory of the particle was measured. A theoretical model of a capsule travelling in static air was derived to predict the trajectory. It estimates closely the distance of projection of particles. Since it has been developed on a real basis such as the mechanism of disintegration for beads formation, slippage of liquid on the surface, radial velocity of the formed droplet at the edge of the disc and has taken into account interactions between the surrounding air, the atomised liquid and rotating disc characteristics, it can be used to predict the trajectory of beads produced by any type of rotating disc and atomised liquid. This model can also help to determine a surface productivity parameter of such system on an industrial scale.

Keywords: Microencapsulation; Atomisation; Rotary disc; Droplets trajectories; Modelling

1. Introduction

The disintegration of liquid into small droplets have long been a significant field of research interest, mainly for two purposes: (1) to apply to a liquid in some unit operations (particularly drying, cooling or freezing) and to enhance their performances by the high specific surface offered by small droplets (Masters, 1988). (2) To produce granular materials that offer some advantages such as stability for encapsulated fragile material or liquid, easier handling and processing and so on.

This disintegration of liquid into droplets is used today for microencapsulation where a core material is inserted or engulfed in a matrix for a wide range of reasons: to protect the core material, improve the product overall or facilitate the production process. The first capsules were created during the fifties for carbon paper (Arshady, 1992), to insert ink into small particles that could explode with the small pressure of a pen. Nowadays, encapsulation offers a big potential application in all areas: pharmaceutical, detergents, cosmetic and food (Brazel, 1999; Gibbs, Kermasha, Alli, & Mulligan, 1999).

Many studies have been done to develop new encapsulated methods and products with sophisticated

* Corresponding author. Fax: +33 2 5178 5454.
E-mail address: teunou@enitiaa-nantes.fr (E. Teunou).

0260-8774/$ - see front matter © 2004 Elsevier Ltd. All rights reserved.
doi:10.1016/j.jfoodeng.2004.10.048

Nomenclature

C_d	drag coefficient (–)
d	diameter of the droplet (m)
d_{50}	the median diameter of the distribution (50% of droplets are under or over this size) (m)
D	diameter of the disc (m)
F_v	feed rate (m^3/s)
g	Standard acceleration of gravity (m/s^2)
h	thickness of the liquid paraffin on the disc (m)
r	radius from the center of the disc (m)
Re	Reynolds number
S_m	minimum surface required for beads production (m^2)
V	velocity of the droplet as it leaves the disc (m/s)
V_r	radial velocity (m/s)
V_t	tangential velocity (m/s)
V_x	horizontal velocity of the droplet as it leaves the disc (m/s)
V_y	vertical velocity of the droplet as it leaves the disc (m/s)
V_0	Initial horizontal velocity = the tangential velocity of the droplet as it leaves the disc (m/s)
$X_{exp.}$	experimental mean horizontal distance on the tray travelled by the bead (m)
$X_{theo.}$	theoretical horizontal distance on the tray travelled by the bead (m)
Y	height of the disc from the collecting tray (m)
Z	number of droplet formation points (–)
μ_a	air viscosity (Pa s)
μ_s	paraffin viscosity (Pa s)
Π	productivity per unit surface (kg/S m^2)
ρ_s	paraffin density (kg/m^3)
ρ_a	air density (kg/m^3)
ω	rotation speed of the disc (rpm)
ω_0	initial rotating speed of the disc (rpm)

functional properties (Diezak, 1988). Some encapsulation methods are: emulsification, fluid bed coating, coacervation, liposomes, complexation, crystallisation, polymerisation, spray drying, cooling and chilling (Risch, 1995, chap. 1). Most of these methods require the disintegration of a liquid, which can be done by a large number of techniques such as pressure atomisation by pressure nozzles or two-fluid, gas-stream atomisation usually with air or steam as the atomising fluid. Atomisation by fast rotating disc, cups and nozzles, centrifugal extrusion and atomisation by longitudinal vibrations audio frequencies is also becoming more and more common.

Among all these, apart from jet cutting, atomisation by rotating disc is the most promising for the food industry because the atomisation conditions are mild, there is no problem of plugging, the process is continuous and power cost are generally low. Rotary atomisation can be defined as a disintegrating system where the feed liquid is distributed centrally on a wheel, disc or cup, and centrifugally accelerated to a high velocity before being discharged as droplets into the surrounding air–gas atmosphere.

The principal objectives in disc design are to ensure that the liquid comes to disc speed and to obtain a uniform drop size distribution in the atomised liquid. Disc diameters vary from 5 cm in small laboratory models to 40 cm for industrial size dryers. Disc speeds range from 1000 to 50000 rpm (Marshal & Vasishtha, 2001). The high speeds are usually used only in small diameter dryers, while in industrial dryers, speeds range from 4000 to 20000 rpm depending on disc diameter and the desired degree of atomisation. Centrifugal disc atomisation is particularly useful with suspensions and pastes that often erode or plug nozzles (Schlameous, 1995, chap. 9). Thick pastes and even particles can be handled if positive pressure pumps are used to feed them to the disc (Sparks, Jacobs, & Mason, 1994, chap. 8). Discs may be operated over a range of feed rates and disc speed without producing excessive variations in the product. The centrifugal disc may be driven by any suitable means; however, high-speed electric motors are preferred at present.

Rotary atomisation has been widely studied and today it is well known that the degree of atomisation depends on the speed, feed rate, liquid properties (viscosity and surface tension) and atomiser design. The readjustment of shear stresses within the liquid once the droplet is airborne is another factor contributing to further disintegration of the droplet (Chicheportiche, 1993). The atomisation mechanisms are still not fully understood because it is a chaotic event. Much of the uncertainty results from the experimental difficulties involved.

But, unfortunately, there is practically no studies or almost no publication on the area required for the collection of beads or particles from the rotating disc in good conditions. That is why the main objective of this paper is focussed on this topic, i.e. the trajectory of the droplet from the disc. This aspect is very important for its application on an industrial scale. The reason for the lack of studies on this topic can be simply explained by the fact that this type of disintegration was applied for spray drying, cooling or freezing, where the shape or the quality of the particle structure was not too important. Indeed, in this case, a small cylindrical chamber,

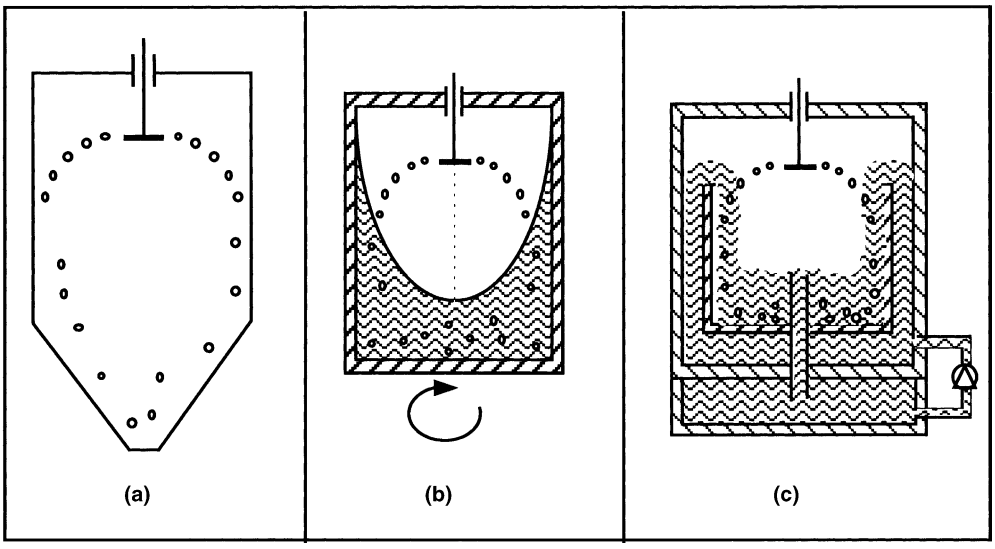

Fig. 1. Different atomising chambers for droplets or particle collection: (a) classical atomising chamber for particles; (b) liquid vortex by rotating vessel, Ogbonna et al., 1989; (c) liquid wall by pumping the liquid (just designed).

where the walls block particles, was sufficient and this small vessel could easily be sterilised (Fig. 1a). But for microencapsulation purpose, the capsule shape and structure are important in such a way that no wall should block the formed particles or the droplets in their trajectory, especially for molten or reservoir capsules. Any blockage of the capsule in the area close to the rotating disc, where the capsule velocity is higher, may results in severe damage to the capsule. On a laboratory scale, the design of a liquid wall such as vortex (Fig. 1b, Ogbonna, Matsumura, Yamagata, Sakuma, & Kataoka, 1989) or liquid pumping (Fig. 1c) can be sufficient providing some surface tension agent such as Tween that will reduce the droplet impact on the liquid wall.

To study the space required for such an operation, a rotating disc atomiser was used to produce paraffin beads and the distance travelled by them from the rotating disc was measured. Theoretical modelling for particle trajectory prediction followed these measurements. A productivity parameter was defined for the collecting surface in order to evaluate the performance of such a system for industrial applications.

2. Materials and methods

2.1. Material

The material used was paraffin (poliwax, Labosi-France) because of its physico-thermal properties. Indeed, the melting point of the bulk paraffin used was equal to 54 °C, i.e. the fine droplets formed by disintegration of hot liquid paraffin could solidified just by contact with air at room temperature and collected as solid particles. The density of the paraffin was 900 kg/m^3. The paraffin viscosity at the processing temperature (60 °C) was 0.0158 Pa s.

2.2. The rotating disc atomiser

The rotating atomiser system used during these experiments was built in our laboratory. It consists of a rotating disc (diameter $D = 0.050$ m) mounted on a motor, a feeding system (two magnetic stirrer/heaters, two beakers, a peristaltic pump and a nozzle) (Fig. 2). A flat tray with compartments (Fig. 2), divided into

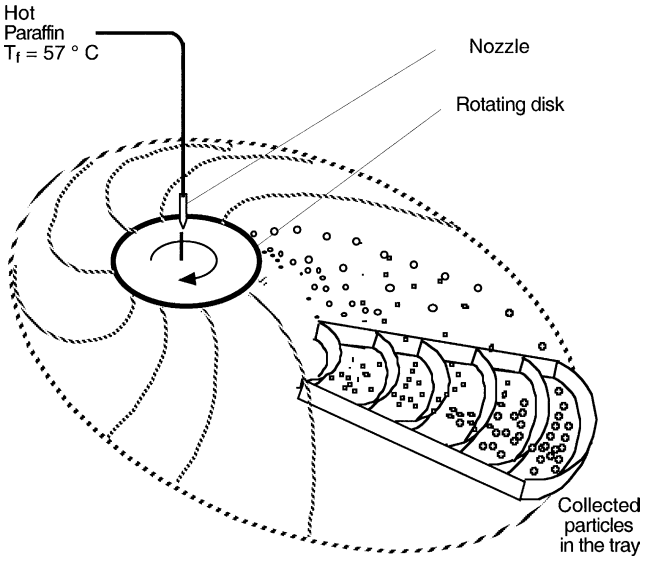

Fig. 2. Schematic presentation of the spinning disc atomiser.

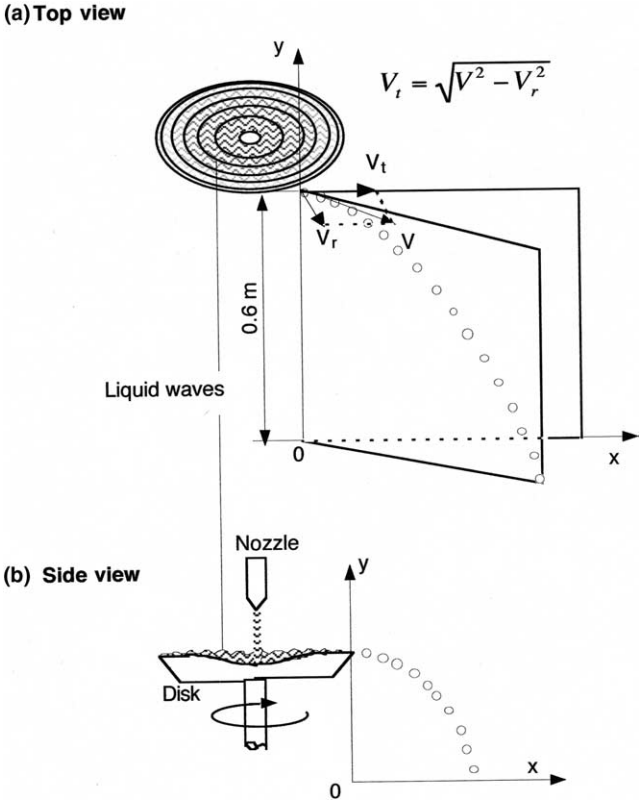

Fig. 3. Disk feeding and liquid waves on the disk.

six parts of 0.20 m length each, was positioned to collect particles or beads of different sizes at different distances. It has a length of 1.2 m to cover the largest distance of projection of the paraffin beads.

The feeding system and the disc was preheated in order to avoid any solidification of the paraffin. Once this is done, the hot melted paraffin (63 °C) was fed by the peristaltic pump (at a rate, $F_v = 2.5$ ml/s) to the top of the rotating disc, which was rotated by the motor at various rotating speeds (0–2000 rpm). As soon as the melted paraffin reached the edge of the rotating disc after spreading to its surface, it disintegrated into droplets, which were projected in the room. Samples of beads were collected in the flat-compartmented collecting vessel after solidification by cooling at room temperature (~20 °C). Note that the temperature of 63 °C was chosen to guarantee a droplet temperature slightly larger than 54 °C (the solidifying temperature).

For each experiment, first, the rotating speed, ω, was fixed and the disc is positioned at a fixed height, $Y = 0.6$ m for travel studies (this distance was chosen after preliminary experiments to allow the paraffin droplets to solidify before landing in the collecting tray). Then, the beads were produced as described above. The mean distance, X, between the edge of the disc and different classes of beads, collected in the flat-compartmented vessel, was measured. Sufficient amounts of paraffin beads samples were withdraw from each compartment for further analysis.

The density and the viscosity of the liquid paraffin were measured respectively by weighing a known volume and using a viscometer (Haake VT500-MVDIN). The diameters of the beads were measured by light diffraction using a Malvern master sizer. The shape of the beads was examined using a microscope coupled with a computerised image analyser.

3. Results and discussion

The manufacturing conditions were $Y = 0.60$ m for the disc height, 2000 rpm for the rotating speed and 2.5 ml/s for the feed rate. The resulting paraffin beads were all spherical as can be seen in Fig. 4. The beads were spread in different compartments and the size analysis of beads collected in each compartment showed that there was a small distribution within each compartment as illustrated by the particle size distribution of the fourth compartment ($d = 580$ μm) (Fig. 5). Despite the effort to narrowing the dispersion, only polydisperse particles could be obtained as shown by the global distribution in Fig. 5. So, for particle travel studies, each compartment was characterised by its mean size (d in micrometer) and the mean distance from the disc ($X_{exp.}$) (see Table 1).

3.1. Mechanisms of bead formation

Some preliminary experiments were carried out in order to describe the mechanisms of liquid disintegration with a rotating disc atomiser; When the liquid reaches the surface of the rotating disc, it is subject to centrifugal

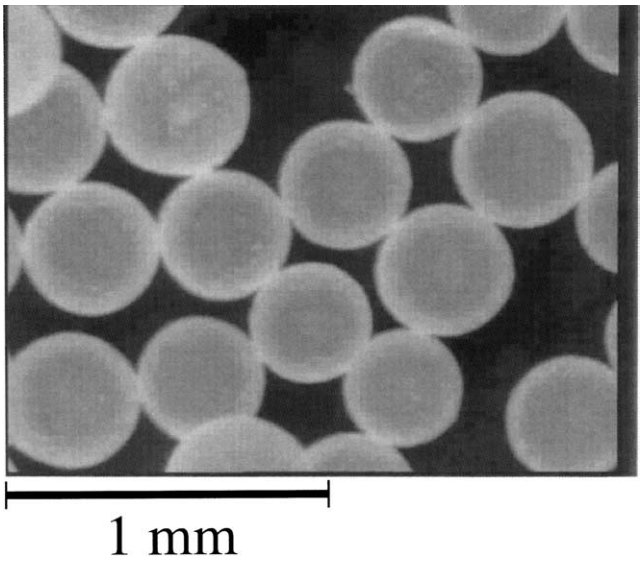

Fig. 4. Photomicrograph of paraffin beads.

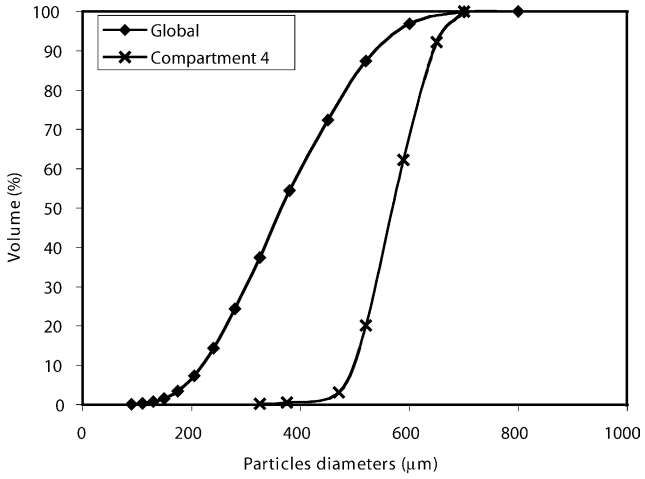

Fig. 5. Particle size distribution of the global beads collected and of the beads collected in compartment 4.

Table 1
Experimental and theoretical distances of bead projection

Diameter (µm)	$Y_{exp.\&theo.}$ (m)	$X_{exp.}$ (m)	$X_{theo.}$ (m)	t (s)
245	0.60	0.19	0.20	0.78
310	0.60	0.30	0.33	0.64
434	0.60	0.50	0.55	0.50
580	0.60	0.70	0.77	0.44
745	0.60	0.90	0.97	0.42

force and extends over the rotating surface as a thin film (Hinze & Milborn, 1950). This was the case when using water or sufficiently hot paraffin, but if the hot liquid paraffin temperature is too close to the melting temperature, it extends as waves as shown in Fig. 6. Three mechanisms of beads formation were observed:

– At any rotation speed of the disc (N) and low volumetric flow rate of the hot water or the hot liquid paraffin, direct drop formation was observed at the edge of the disc as shown diagrammatically in Fig. 6a. The number of points of formation of droplets at the edge of the disc could be counted ($Z \sim 70$). The collected paraffin beads showed a large particle size distribution (Fig. 5). This is probably due to the fact that at low feeding rates and disc speeds, sprays consist of two, three or more prominent droplet sizes, i.e. parent droplet and some satellites (Fig. 6a). The vibration of the system and variations of the paraffin flow rate, Q, amplify this phenomenon.
– With increasing volumetric flow rate, there was a transition from the direct droplet formation to a ligament type of disintegration. The ligaments begin to extend out from the edge of the disc and their length increased with an increase in Q until they split themselves into parents and satellites droplets as shown in Fig. 6b.
– Higher feed rate results in the merging of different ligaments to form a liquid sheet, which appears around the disc edge, and disintegrate (Fig. 6c).

Note that for the present experiments, with a maximum flow rate of 2.5 ml/s, and a maximum rotating speed of 2000 rpm, only the first mechanism (direct formation) was observed during the investigation of the paraffin beads trajectory. It must also be recalled that only the disintegration by direct formation (Fig. 6a) and by ligament formation (Fig. 6b) can lead to monodisperse beads if and only if the liquid is fed to the disc surface in a laminar and stable way (Masters, 1988). That was not the case during these experiments, and this explains why a large particle size distribution was observed, due to the shaky feeding system. Some improvements have been done for this purpose, notably the use of a double head peristaltic pump to reduce pulses and the forming of a small hollow (60 mm^3) on the disc surface to minimise the effect of theses pulses.

3.2. Experimental trajectory of paraffin beads

The trajectory of the beads was assessed by interception of the beads, at different positions of the tray, with a vertical paper wall, followed by the measurement of the height $Y_{exp.}$ of the mark made by the droplet (value is reported in Table 1 and on the graph of Fig. 7). It appears from this graph that, as was expected, the trajectories of beads are parabolas and that the mean distance of projection ($X_{exp.}$) increases with an increasing bead mean size.

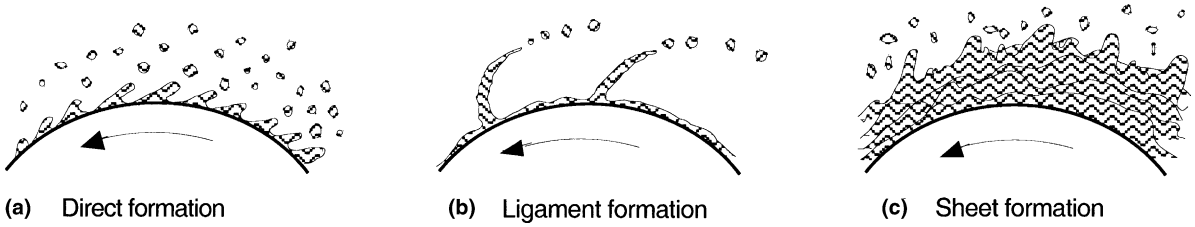

Fig. 6. Mechanisms of droplet formation by rotating disk atomisation.

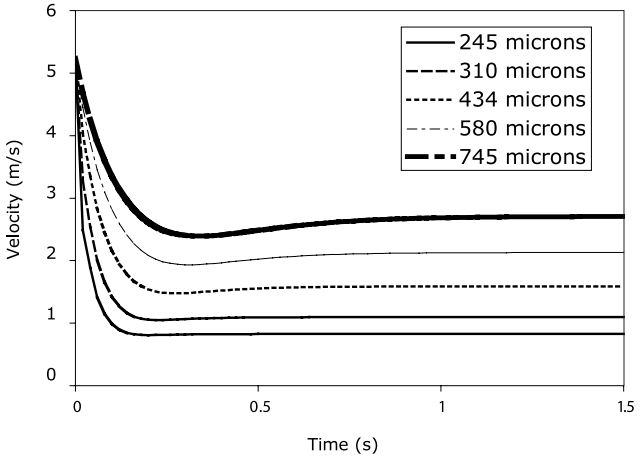

Fig. 7. Particles velocities versus time.

3.3. Theoretical prediction of paraffin beads trajectory

3.3.1. Modelling

Modelling here consists in determining:

- The trajectory of the droplet, i.e. the distance, x from the edge of the disc travelled by the droplet versus the height of the disc, y.
- The vertical and horizontal components of the droplet velocity, which are important for assessing the collecting conditions, and avoiding splitting of droplets by violent impacts.
- The travelling time of the droplet. This parameter is important for optimising the quality of the beads in the case of hot melt, since the cooling time must be lower than the travelling time.

3.3.2. Assumptions

The trajectory of a droplet leaving the disc depends on a lot of factors (environmental and technical) that are very difficult to take in account together. Some assumptions are therefore necessary to simplify this analysis.

- No interaction between droplets (considered as single particles).
- Direct bead formation process (Fig. 6a).
- The beads are spherical.
- The trajectory of a droplet is located in a vertical plane tangential to the disc (i.e. the radial velocity is neglected).
- The initial droplet velocity at the edge of the disc is taken equal to the peripheral tangential velocity of the disc (no slippage of liquid on the disc surface).

So, if a spherical droplet (diameter d) is considered leaving the rotating disc (diameter D) at the velocity V in the plane (x, y) as shown in Fig. 3, the two components of the droplet velocity can be written as

$$\begin{cases} \dfrac{dx}{dt} = V_x(t) \\ \dfrac{dy}{dt} = V_y(t) \end{cases} \quad \text{At } t = 0 \quad \begin{cases} x = 0 \\ y = 0.6\ \text{m} \end{cases} \tag{1}$$

$$V = (V_x^2 + V_y^2)^{\frac{1}{2}} \tag{2}$$

Taking into account the air friction, which slows down the particles in their trajectory and assuming no slippage on the disc ($V_s = 0$), the derivative of the velocity leads to

$$\begin{cases} \dfrac{dV_x}{dt} = -\dfrac{3}{4} \cdot \dfrac{\rho_a}{\rho_s} \cdot \dfrac{C_D}{d} \cdot V \cdot V_x \\ \dfrac{dV_y}{dt} = -g - \dfrac{3}{4} \cdot \dfrac{\rho_a}{\rho_s} \cdot \dfrac{C_D}{d} \cdot V \cdot V_y \end{cases} \tag{3}$$

$$\text{At } t = 0 \quad \begin{cases} V_x = V_t - V_s = V_0 \\ V_y = 0 \end{cases}$$

where C_D is the drag coefficient, which is proportional to the total drag force exerted by air on the beads.

The simulation of Reynolds number using Eq. (4) and calculated for different experimental conditions shows that the Reynolds numbers were all between 65 and 300.

$$Re = \frac{\rho_a \cdot V \cdot d}{\mu_a} \tag{4}$$

Therefore Eq. (5) was used to calculate the drag coefficient C_D since this equation represents the drag coefficient expression for Reynolds numbers between 65 and 300 (Geankoplis, 1993).

$$C_D = \frac{24}{Re}\left(1 + \frac{Re^{\frac{2}{3}}}{6}\right) \tag{5}$$

The two first order non-linear coupled differential equations (Eq. (3)) were solved numerically, since they could not be solved analytically.

The numerical resolution provides X and Y values (Table 1) that will be used here to plot the trajectories of droplets or particles. The travelling time, required by the particle to travel from the disc edge to a given point, is very short in all cases (less than a second), indicating how fast solidification should take place. This also indicates that particles travel very fast, even if the velocity of particles at various sizes (Fig. 7) in all case decreases, due to air friction, quickly from the initial velocity V_0, to a minimum before it levels off in less than a half-second. After this half second the kinetic energy that causes damage during any impact is almost constant and small. Note that the droplets must be collected in the area corresponding to the minimum velocity in

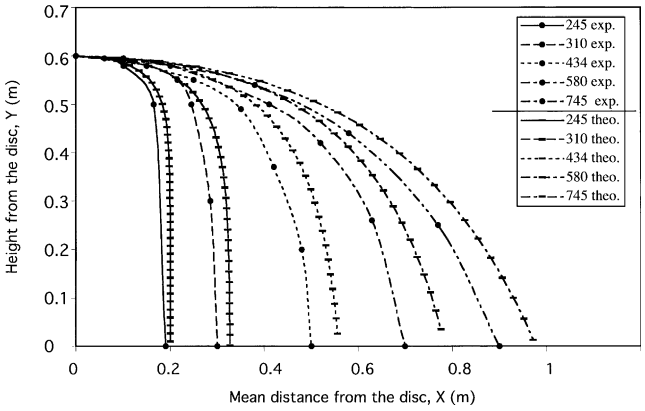

Fig. 8. Experimental and theoretical bead trajectories.

order to reduce percussions or impacts at the collecting point, which can affect the quality of the beads.

The curves (Fig. 8) and distances (Table 1) of X versus the height Y given by the theoretical model for various beads sizes are close to those obtained experimentally, especially for larger particles and this confirms that the air friction contributes a lot in slowing the droplet in its trajectory. The difference between those two curves can be summarised as a slight overestimation of the distance X by the theoretical model. The roots of this difference lays at the beginning, i.e. when the droplet lefts the disc. Indeed, the initial droplet velocity is overestimated probably because of some assumptions mentioned above. Let examine some of them:

(1) There is slippage of the melted paraffin on the disc surface.

When a flat and smooth disc is rotating at high speed, if a liquid is fed on to its top surface, severe slippage occurs between the feed liquid and the disc due to air friction (Fig. 9). The velocity of liquid from the edge of the disc is much lower than the peripheral speed of the disc. Even if the very low speed in this case (2000 rpm) is adequate for no slippage, it seems, according to Fig. 8 that the theoretical initial velocity is overestimated.

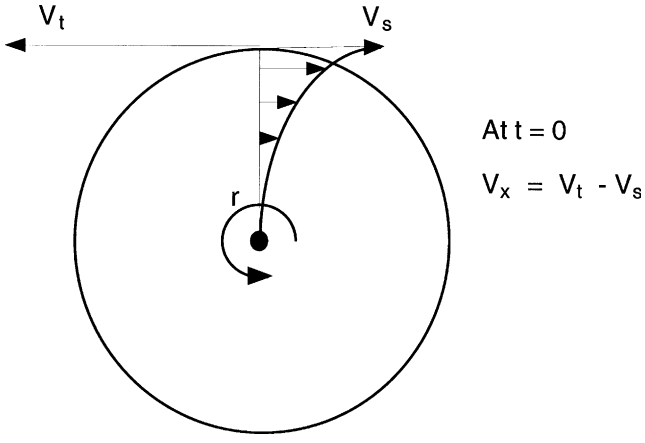

Fig. 9. Slipping velocity of the hot paraffin oil on the disc, due to air friction.

Applying the boundary layer theory for a laminar regime, the slipping velocity, V_s, was calculated by iteration using Eq. (6) (from Schlichting & Gersten, 2000).

$$V_s(r) = \frac{3.87h \cdot \gamma_a^{\frac{1}{2}} \cdot \rho_a(\omega_0 - \omega)^{\frac{3}{2}} \cdot r^2}{2\pi\mu_s} \tag{6}$$

The calculated value of this velocity at the edge of the disc (i.e. for $r = D/2$) is $V_s = 0.52$ m/s, representing about 10% of the tangential velocity ($V = 5.23$ m/s), showing that neglecting the slippage at the disc surface was not a good approximation. Also, to prevent slippage in commercial atomisers, radial vanes are used. The liquid is confined to the vane surface, and at the periphery the possible maximum liquid release velocity is attained. The value of V_s will then be removed from the peripheral velocity to correct the initial velocity of the droplet from the edge of the disc. That means Eq. (3) should now be solved with the following boundary conditions:

$$\text{At } t = 0 \quad \begin{cases} V_x = V_t - V_s = V_0 - V_s \\ V_y = 0 \end{cases}$$

(2) The radial velocity is not negligible (i.e. the trajectory of a droplet is not located in a vertical plane tangential to the disc).

The radial droplet velocity was calculated using Eq. (7):

$$V_r = \frac{F_v}{2\pi R \cdot h} \tag{7}$$

where h is the thickness of the liquid layer sliding on the surface of the disc. h was approximated by a measure of the solidified paraffin on the surface of the disc when stopping the experiment. Eq. (7) was derived assuming that the feeding flow rate equals the rate of droplets formation (flow rate conservation). The value of V_r, calculated with $h = 42$ μm, is 0.37 m/s (representing about 7% of the initial tangential velocity $V = 5.23$ m/s), seems not negligible in magnitude but its effect on this tangential velocity, evaluated by the boundary conditions below, is negligible (see the computed values of velocities in Table 2). Neglecting the radial velocity is generally considered as a good assumption for such a problem and this has been used successfully by Yang and Schrock (1993) in their works. Nevertheless, this value will be

Table 2
Initial velocity under various assumptions conditions

Assumptions		Tangential velocity of the droplet at $t = 0$
Slippage on the disc	Radial velocity	V_x (m/s)
No	No	5.23
Yes	No	4.71
Yes	Yes	4.69

taken into account in this case because the tangential velocity is small ($V = 5.23$ m/s). A new value of V_t in the X–Y plane must then be calculated (see Fig. 3). The boundary conditions for Eq. (3) become:

$$\text{At } t = 0 \quad \begin{cases} V_x = V_t - V_s = \sqrt{V_0^2 - V_r^2} - V_s \\ V_y = 0 \end{cases}$$

So, after corrections, the calculated values of V_x at $t = 0$ are summarised in Table 2.

Applying these corrections bring the theoretical curves close to the experimental (Fig. 10) and the predicted distance of projection of the beads match more closely with the experimental distances (Table 3).

The little difference that can be observed may be due to the fact that the model is calculated for a single and isolated droplet. This assumption is not correct too since a large distribution of particles was observed. This distribution can have an impact on the droplets trajectories; the turbulence generated by different particles brings interaction between different droplets, slowing them down. The smallest ones are more influenced in their trajectories and the length of time that they need to reach the collecting tray indicates that they are more affected by air friction (Table 1).

Also note that, during their travel, the paraffin droplets change in state, solidifying after cooling. This transition may also be added as an argument to justify the short difference observed after correction.

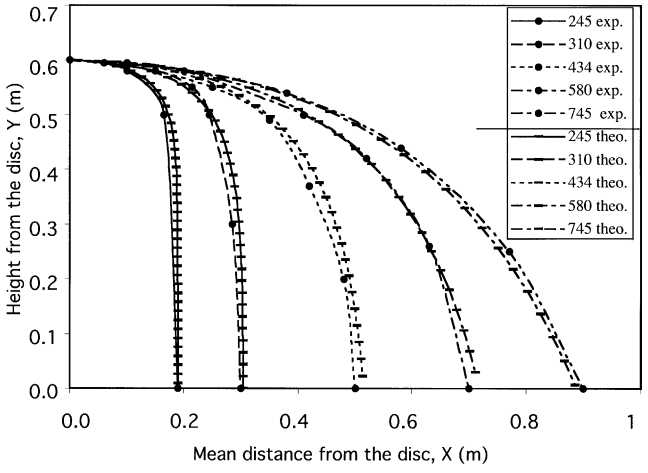

Fig. 10. Experimental and corrected theoretical bead trajectories.

Table 3
Some experimental and theoretical data

Diameter (μm)	Y (m)	$X_{exp.}$ (m)	$X_{theo.}$ (m)	$X_{theo.}$ (m) corrected	Π (m^2/kg/s)
245	0.60	0.19	0.20	0.20	42
310	0.60	0.30	0.33	0.31	105
434	0.60	0.50	0.55	0.52	277
580	0.60	0.70	0.77	0.73	529
745	0.60	0.90	0.97	0.91	829

3.4. Productivity of the rotating disc

Regarding particle trajectories, many types of productivity characteristics can be defined. Here, we define a productivity parameter ($\Pi_{(D,\omega,F_v)}$) which is the minimum surface required to produce beads with a given diameter using Eq. (8). The index (D, ω, F_v) indicates that this productivity rate is calculated for a given disc diameter, rotation speed and the flow rate. This parameter allows estimation of the surface required for given production characteristics and evaluation of X, Y by modelling can be for a great help for this purpose.

$$\Pi_{(D,\omega,Q_v)} = \frac{S_m}{Q_v \cdot \rho_s} = \frac{\pi(D + 2X)^2}{4Q_v \cdot \rho_s} \tag{8}$$

For a constant rate and velocity, the minimum surface required for bead production (kg/s) appears to be very important (Table 3). The rotating disc atomisation for microencapsulation application is definitely a space consuming technique. This surface increases logically when bead size increases.

4. Conclusion

Rotating disc atomisation gives, as is shown above, beads of wide range of particles size. It has the advantage that it can be scaled up easily. For example for larger production, higher flow rates can be used with bigger discs and higher speeds. So, it is a good system that can be used efficiently in the industries for microencapsulation of liquid and solids using polymer solutions and hot melts. But the main drawback of this method is the required surface or volume necessary to collect the formed beads in good conditions as indicated by the performance defined here in terms of the minimum surface ($\Pi_{(D,\omega,F_v)}$). This necessity to define the productivity of an encapsulation process in terms of m^2/kg is valid for all types of liquid disintegration techniques by a rotating tool such as centrifugal extrusion, rotating cup, disc or wheel.

Finally, the theoretical simplified model of particle trajectory that was obtained by various assumptions can be considered as close to the experimental curves. The difference between the two curves for smaller particles can be attributed completely to interaction between particles and the uncertainty on the various measured values (velocities, viscosity, mean particle size, etc.).

The perspectives of this work are really opened because in addition to deriving a general equation giving X and Y as a function of d_p, F_v, ρ_s, ρ_a, D, h, ω, Re, μ_s, etc., there is a real possibility of developing a suitable

experimental tool to produce monodispersed beads. This could be completed by experimental measurement of particle velocity that can be done by high-speed photography, particle velocity probes or sounds transducers.

Acknowledgment

The authors would like to thank N. Benard, M. Lauvergeon, V. Tessier for their contribution and O. Rioux, for their technical assistance.

References

Arshady, R. (1992). Microcapsules for food. *Journal of Microencapsulation*, 415–455.

Brazel, C. S. (1999). Microencapsulation: offering solutions for the food industry. *Cereal Food World, 44*(6), 388–393.

Chicheportiche, J. M. (1993). *Etude de la fragmentation commandée des jets liquides issus d'un disque en rotation et réalisation d'un générateur de gouttelettes monodispersées*, Paris, p. 205 (Doctorat de l'Université Pierre et Marie Curie: 5 mai 1993).

Diezak, J. (1988). Microencapsulation and encapsulated ingredients—use of microencapsulation can improve ingredient functionality. *Food Technology*(April), 136–151.

Geankoplis, C. J. (1993). *Transport processes and unit operations* (3rd ed.). Englewood Cliffs, NJ: Prentice hall, Inc. (pp. 116–119).

Gibbs, B. F., Kermasha, S., Alli, I., & Mulligan, C. N. (1999). Encapsulation in the food industry: a review. *International Journal of Food Sciences and Nutrition, 50*(3), 213–224.

Hinze, J. O., & Milborn, H. (1950). Atomization of liquids by means of rotating cup. *Journal of Applied Mechanics*(June), 145–153.

Marshal, M., & Vasishtha, N. (2001). Market place of microencapsulation in North America, 2nd Industrial Technological Trade Fair in Micro- & Bio-encapsulation, Nantes, France.

Masters, K. (1988). Drying of droplets/sprays. In *Spray drying handbook* (pp. 298–342). New York: Longman Scientific and Technical, J. Wiley and Sons.

Ogbonna, J. C., Matsumura, M., Yamagata, T., Sakuma, H., Kataoka, H., et al. (1989). Production of micro-gel beads by a rotating disc atomizer, University of Tsukuba, Tokyo. *Journal of Fermentation and Bioengineering, 68*(1), 40–48.

Risch, S. J. (1995). *Encapsulation: Overview of uses and techniques*. In: 0097-6156/95/0590-0002$12.00/0 (pp. 1–7). American Chemical Society.

Schlameous, W. (1995). Centrifugal extrusion encapsulation. In S. J. Risch (Ed.), *Encapsulation and controlled Release of food ingredients* (pp. 100–103). American Chemical Society.

Schlichting, H., & Gersten, K. (2000). *Boudary layer theory*. Berlin, Germany: Springer Verlag (p. 799).

Sparks, R. E., Jacobs, I. C., & Mason, N. S. (1994). *Centrifugal suspension-separation for coating food ingredients*. In: 0097-6156/95/0590-0087$12.00/0 (pp. 87–95). American Chemical Society.

Yang, Y., & Schrock, M. D. (1993). Image transformation method for determining kernel motion positions in three dimensions. *Transactions of the ASAE, 36*(4), 1229–1234.